Pure appl. geophys. 157 (2000) 1663–1681
0033–4553/00/101663–19 $ 1.50 + 0.20/0

Pure and Applied Geophysics

Accelerated Preshock Deformation of Broad Regions in the Aegean Area

B. PAPAZACHOS[1] and C. PAPAZACHOS[1]

Abstract—Twenty-four regions where accelerating deformation has been observed for a few decades before corresponding strong ($M = 6.0–7.5$) mainshocks are identified in the broader Aegean area. To a first approximation these preshock regions have elliptical shapes and the radius, R (in km), of a circle with an area equal to the corresponding ellipse is related to the moment magnitude, M, of the mainshock by the equation:

$$\log R = 0.42M - 0.68.$$

The dimension of each preshock region is about seven to ten times larger than the rupture zone (fault length) of the corresponding mainshock. The time variation of the cumulative Benioff strain was satisfactorily fitted by a power-law relation, which is predicted by statistical physics if the mainshock to which accelerating strain rates leads is considered as a critical point. The duration, t (in years), of the accelerating Benioff strain release period is given by the relation:

$$\log t = 5.94 - 0.75 \log s_r$$

where s_r is the mean Benioff strain rate release (per year for 10^4 km^2) in the preshock region calculated by the complete available data ($M \geq 5.2$) for the entire instrumental period (1911–1998). The importance of identifying and investigating such regions for better understanding the dynamics of the active part of the lithosphere as well as for earthquake prediction and time-dependent seismic hazard assessment is discussed.

Key words: Accelerated preshock deformation, Benioff strain, critical phenomena, Aegean area.

Introduction

Research work of the last four decades has shown that intermediate magnitude seismicity increases before large earthquakes in relatively broad regions (TOCHER, 1959; MOGI, 1969; RALEIGH *et al.*, 1982; KEILIS-BOROK *et al.*, 1988; LINDH, 1990; KNOPOFF *et al.*, 1996). It has been further observed that large earthquakes follow periods of accelerating regional seismicity and that the time variation of this preshock seismicity can be quantified by power-law relations (BUFE and VARNES, 1993; BREHM and BRAILE, 1998; 1999; JAUMÉ and SYKES, 1999). This behavior of

[1] Geophysical Laboratory, Aristotle University of Thessaloniki, PO Box 352-1, GR-54006, Thessaloniki, Greece. E-mail: basil@lemnos.geo.auth.gr, costas@lemnos.geo.auth.gr

the preshock seismic activity can be explained by principles of statistical physics, that is, by considering the process of generation of these moderate magnitude shocks (preshocks) as a critical phenomenon, culminating in a large event (mainshock) considered as a critical point (SORNETTE and SORNETTE, 1990; ALLÈGRE and LE MOUEL, 1994; SORNETTE and SAMMIS, 1995). Such behavior is also supported by recent observations which indicate that rupture in heterogeneous media is a critical phenomenon (VANNESTE and SORNETTE, 1992; LAMAIGNERE *et al.*, 1996; ANDERSEN *et al.*, 1997).

The results of the above-mentioned research work, based on seismological observations as well as on statistical physics and rock mechanics, encouraged some seismologists to propose methods for predicting the time and magnitude of a mainshock by fitting power-law equations to the time variation of some measures (seismic moment rate, Benioff strain rate, etc.) of the preshock seismicity (SYKES and JAUMÉ, 1990; BUFE and VARNES, 1993; BUFE *et al.*, 1994; BREHM and BRAILE, 1998, 1999). Thus BUFE and VARNES (1993) used the cumulative Benioff strain, $S(t)$, as a measure of the preshock seismicity at time t, defined as

$$S(t) = \sum_{i=1}^{n(t)} E_i(t)^{1/2} \tag{1}$$

where E_i is the seismic energy of the ith preshock and $n(t)$ is the number of events at time t. To fit the time variation of the cumulative Benioff strain, they proposed a relation of the form:

$$S(t) = A + B(t_c - t)^m \tag{2}$$

where t_c is the origin time of the mainshock and A, B, m are parameters which can be calculated by the available observations. B is negative, m is positive and smaller than 1 and A is the total Benioff strain including the strain of the mainshock (VARNES, 1989). Since the seismic energy can be calculated from the magnitude of the earthquakes, data can be used to determine the parameters of relation (2) and to estimate the origin time of the mainshock and its magnitude. In practice, however, there are several difficulties for such a prediction, one of which is the accurate identification of the preshock (critical) region.

Recently BOWMAN *et al.* (1998) presented a systematic procedure to test for accelerating seismicity patterns and to identify regions approaching criticality before all earthquakes with $M \geq 6.5$ which occurred along the San Andreas fault system since 1950. To quantify the degree of acceleration of the Benioff strain, they defined a curvature parameter, C, as the ratio of the root-mean-square error of the power-law fit (relation 2) to the corresponding linear fit error. Therefore, this parameter is less than 1 for accelerating or decelerating seismicity and equal to 1 for linear variation of seismicity. To identify the critical region for each of these earthquakes they developed an optimization algorithm which identifies regions of accelerating seismicity by examining the value of C in circles centered at the

epicenter of the mainshock. The circle for which C had a minimum value and the critical exponent m was less than 0.8 was considered as the critical region for each mainshock. They also found a linear relation between the logarithm of the radius, R, of the critical region and the magnitude of the mainshock with a slope equal to 0.44.

The goal of the present work is to identify preshock (critical) regions in the crust of the Aegean and surrounding area by a similar procedure to that applied by BOWMAN *et al.* (1998) and to investigate the form of the time variation of strain in these regions. Work on the accelerating seismicity before some earthquakes of the Aegean area has already been done by some researchers (PAPADOPOULOS, 1986, 1988; PAPAZACHOS *et al.*, 1999a). The variation of the moderate magnitude shallow seismic activity in this area during a seismic cycle has been investigated by KARAKAISIS *et al.* (1991), using the frequency of shocks and the rate of seismic energy release. These authors also observed a phase of accelerating seismicity before large shocks.

The term ''preshock'' is used in the present paper for the intermediate magnitude shocks which occur in the critical region during the phase of accelerating seismicity which is culminated in the generation of a large earthquake (mainshock). Also ''postshocks'' are the shocks which occur in the critical region during the phase of decelerating seismicity after the generation of the mainshock. Thus preshocks and postshocks last for considerably longer periods and their foci are distributed in a larger region than the classical foreshocks and aftershocks.

The Aegean area is the most active part of western Eurasia. The Aegean lithosphere is located in the front part of the Eurasian lithosphere and is in collision with the eastern Mediterranean lithosphere (front part of the African lithosphere). Its high seismic activity is mainly due to the subduction of the Mediterranean lithosphere under the Aegean, to the westward motion of the Anatolia lithospheric plate and to the very fast motion of the Aegean to the southwest (PAPAZACHOS *et al.*, 1998). Hence, shallow earthquakes as well as intermediate depth earthquakes with focal depths reaching 180 km and magnitudes up to about 8.0 occur in this area. In the present work only shallow mainshocks are considered.

The Data

In the present study only instrumental data were used, that is, epicenters and magnitudes of shallow ($h < 60$ km) earthquakes which occurred in Greece and surrounding area (34°N–43°N, 19°E–30°E) since 1911 when the first reliable seismograph (Mainka type of two horizontal components) was installed in Athens. Thus, earthquakes with $M \geq 4.9$ that occurred in this area since 1911 are fairly well located and their magnitudes are well determined. After World War II, locations of even smaller earthquakes were improved and for this reason parameters of earth-

quakes with $M \geq 4.5$ which occurred in this area since 1950 are also known with satisfactory accuracy.

In 1965 the first network of seismological stations was installed in Greece by the Geodynamic Institute of the National Observatory at Athens. From January 1981, this network was augmented by the installation of the telemetric network of the Geophysical Laboratory of the University of Thessaloniki in northern and later in central Greece. For this reason, accurate information for earthquakes with $M \geq 4.0$ in Greece and the surrounding area is available since 1981. Moreover, the data used are also complete for $M \geq 5.2$ during 1911–1998, $M \geq 4.8$ during 1950–1998 and $M \geq 4.5$ during 1965–1998 (COMNINAKIS and PAPAZACHOS, 1986).

The data for the period 1911–1985 are taken from a published catalogue (COMNINAKIS and PAPAZACHOS, 1986), while for the rest of the period (1986–1998) the data were taken from a new unpublished catalogue of the Geophysical Laboratory of the University of Thessaloniki. The error in the epicenters varies with time and magnitude and is of the order of 10 km for recent earthquakes, although it can reach up to 25 km for the older ones (before 1965). All magnitudes are moment magnitudes, either originally reported or converted from other magnitude scales by appropriate formulas (PAPAZACHOS *et al.*, 1997) and their error is less than 0.3.

The selection of the mainshocks, of which the preshock activity is investigated in the present study, was based on the available data mentioned above and on the observation that the duration of the preshock activity for mainshocks considered in this study is of a few decades. In this way two complete sets of mainshocks were considered. The first set consists of all mainshocks with $M \geq 6.5$ which occurred in this region since 1948 (18 mainshocks) and were preceded by 30 or more known smaller shocks in the excitation area (preshocks). Thus the mainshocks of this set occurred at least 37 years after 1911, when instrumental information for shocks with $M \geq 5.2$ was available. The second set consists of all mainshocks with magnitudes between 6.0 and 6.4 which occurred in this region since 1981 (6 mainshocks) and were also preceded by 30 or more preshocks. Since the first such mainshock occurred in 1986, the mainshocks of this set occurred at least 36 years since 1950, when reliable instrumental information for shocks with $M \geq 4.8$ was available. It is very difficult to identify smaller mainshocks because in active areas like the Aegean these shocks are usually related to larger earthquakes, both temporally and spatially. The minimum number of preshocks was kept high ($= 30$) here in order to secure as much accuracy in the derived relations as possible. Smaller samples, however, can also produce good results but we preferred at this stage to keep a high reliability for the derivation of these relations. The first five columns of Table 1 supply information on the code number, date, origin time, epicenter and magnitude of these 24 shallow mainshocks, and Figure 1 shows the epicenters of these mainshocks.

Table 1

Information on the parameters of the 24 mainshocks and of their preshock regions investigated in the present paper

No.	Date	Or. Time	φ_N^0	λ_E^0	M	z	e	R	t	m	C	N	$M_{\min}$	$\log s_r$
1.	1948,02,09	12:58:13	35.50	27.20	7.1	40	0.80	190	25.1	0.58	0.59	44	5.2	5.95
2.	1952,12,17	23:03:57	34.40	24.50	7.0	20	0.80	171	40.0	0.43	0.38	33	5.2	5.77
3.	1953,03,18	19:06:16	40.02	27.53	7.4	70	0.80	246	33.2	0.40	0.48	37	5.2	5.89
4.	1953,08,12	09:23:52	38.30	20.80	7.2	10	0.60	216	28.6	0.33	0.49	62	5.2	6.16
5.	1954,04,30	13:02:38	39.28	22.29	7.0	90	0.80	171	23.3	0.31	0.35	37	5.2	6.08
6.	1956,07,09	03:11:40	36.64	25.96	7.5	50	0.90	284	36.6	0.52	0.35	100	5.2	5.84
7.	1957,04,25	02:25:42	36.55	28.80	7.2	110	0.75	213	30.3	0.32	0.51	37	5.2	5.91
8.	1967,03,04	17:58:09	39.20	24.60	6.6	90	0.85	106	56.2	0.37	0.45	31	5.2	5.69
9.	1968,02,19	22:45:44	39.50	25.00	7.1	30	0.85	157	50.1	0.27	0.31	36	5.2	5.65
10.	1970,03,28	21:02:23	39.20	29.50	7.1	150	0.80	175	45.2	0.37	0.47	35	5.2	5.74
11.	1972,05,04	21:39:57	35.10	23.60	6.5	110	0.95	89	56.4	0.52	0.59	31	5.2	5.95
12.	1976,05,11	16:59:45	37.40	20.40	6.5	0	0.80	131	13.4	0.61	0.55	38	4.8	6.43
13.	1979,04,15	06:19:41	42.00	19.00	7.1	160	0.95	207	48.3	0.52	0.69	54	5.2	5.85
14.	1981,02,24	20:53:37	38.07	23.00	6.7	120	0.80	128	51.2	0.53	0.60	38	5.2	5.80
15.	1981,12,19	14:10:52	39.00	25.26	7.2	60	0.80	203	28.0	0.43	0.60	129	4.8	5.95
16.	1983,01,17	12:41:31	38.10	20.20	7.0	160	0.80	171	20.0	0.53	0.54	114	4.8	6.28
17.	1986,09,13	17:24:34	37.13	22.09	6.0	120	0.90	73	19.7	0.40	0.25	36	4.5	6.18
18.	1992,04,30	11:44:40	34.99	26.72	6.1	10	0.90	71	19.3	0.57	0.36	103	4.5	6.21
19.	1994,09,01	16:12:42	41.12	21.25	6.1	80	0.95	61	30.7	0.47	0.53	31	4.8	5.88
20.	1995,05,13	08:47:15	40.15	21.68	6.6	30	0.70	127	25.4	0.54	0.48	153	4.5	5.85
21.	1995,06,15	00:15:49	38.36	22.28	6.4	100	0.95	95	11.5	0.55	0.54	66	4.5	6.37
22.	1997,10,13	13:39:00	36.33	22.17	6.4	120	0.80	92	31.8	0.56	0.48	102	4.5	5.99
23.	1997,11,14	21:38:00	38.73	25.91	6.0	30	0.85	65	33.9	0.52	0.66	51	4.5	5.72
24.	1997,11,18	13:07:00	37.58	20.57	6.6	50	0.95	106	13.9	0.70	0.59	138	4.5	6.38

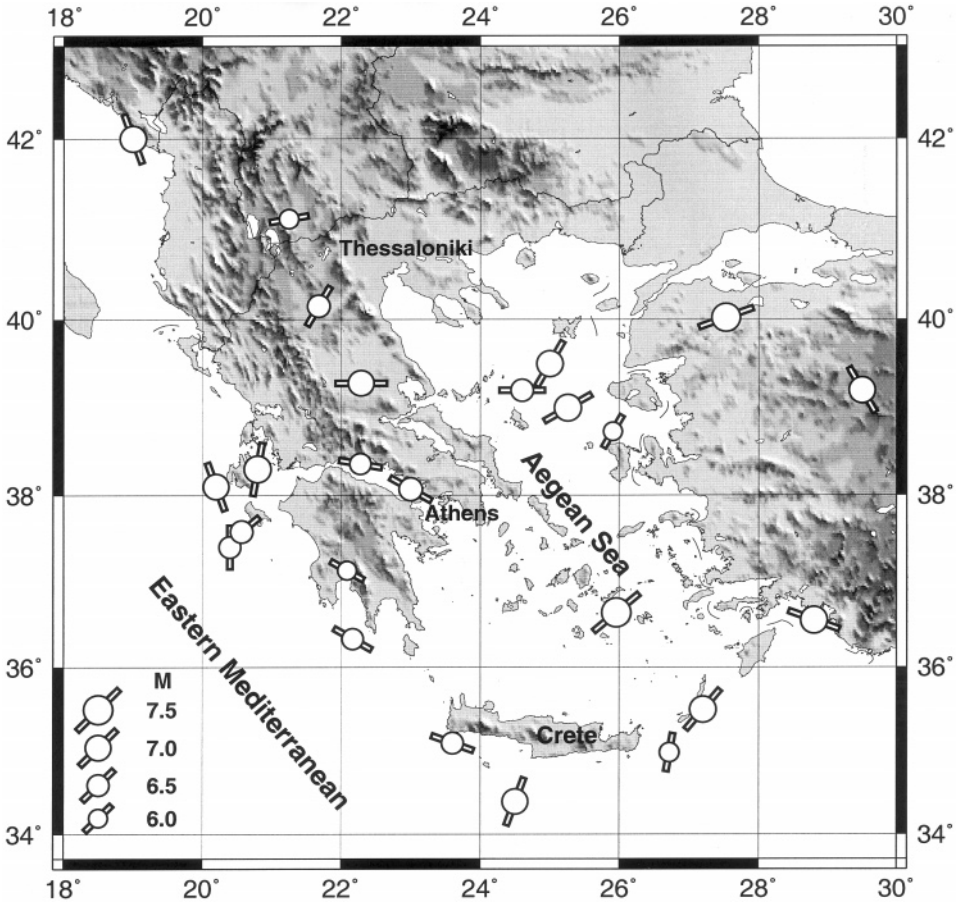

Figure 1
Epicenters of the 24 mainshocks in the Aegean crust for which accelerating Benioff strain has been investigated in their preshock broad regions. The two small lines indicate the direction of the major axis of the corresponding elliptical preshock regions.

The following relation between the moment magnitude, M, and seismic moment, M_o (in Nt.m), has been found to hold for shallow earthquakes in the Aegean area (PAPAZACHOS and PAPAZACHOU, 1997):

$$\log M_o = 1.5M + 9.0. \tag{3}$$

Taking also into consideration that seismic energy, E, is related to seismic moment by the equation:

$$E = 5.0 * 10^{-5} M_o \tag{4}$$

(VASSILIOU and KANAMORI, 1982; KANAMORI *et al.*, 1993), we find the following relation:

$$\log E = 1.5M + 4.7 \quad (5)$$

which has been used to calculate the seismic energy from the moment magnitude, and therefore the Benioff strain (equation 1).

Method Applied

To define the region which has been seismically excited before each one of the mainshocks listed in Table 1, we considered elliptical areas centered in the epicenter of the mainshock. In each case the azimuth, z (measured clockwise from north), ellipticity, e, and the large axis, a, of the ellipses were allowed to vary. All possible azimuths (in 10° steps) were examined, as well as a large number of ellipticity values. Moreover, a broad range of possible distances up to 500 km from the epicenter of the mainshock (in 10 km steps) was also considered. Within each elliptical area defined for each of the previous z-e-a combinations, the cumulative Benioff strain, S, was calculated as a function of time by the use of the magnitudes of the shocks which occurred within the elliptical area using equations (1) and (5), including the mainshock. This estimation was performed for different time periods before the main earthquake by considering different starting times since the onset of the accelerated seismicity period started (in 1-year steps). Therefore, the finally examined data sets were constructed from all possible earthquake catalogues created for each z-e-a-starting year combination.

For each of the previously defined data sets the observed cumulative strain, $S(t)$, variation with time was fitted by a relation of the form (2), allowing the determination of parameters B and m, as well as the root-mean-squares fit error. Since in the present study we wanted to identify the presence of accelerated seismic deformation behavior rather than attempt a prediction, the cumulative Benioff strain released up to (and including) the main earthquake, A, as well as the time of occurrence of this event, t_c, were considered known and fixed. Moreover, the same data were fitted by a linear relation and the corresponding errors were also calculated. The elliptical area for which the ratio, C, of the error of the power-law relation (equation 2) to the error of the linear relation was minimum has been finally considered as the preshock region of each mainshock, as suggested by BOWMAN *et al.* (1998).

Figure 2 shows the variation of the parameter C with the distance (length of the maximum axis of ellipses), a, for three destructive mainshocks with magnitudes $M = 7.5$ (9 July, 1956), $M = 6.0$ (13 September, 1986) and $M = 6.6$ (13 May, 1995). For these plots the finally adopted z-e-starting time values were held fixed and only, a, was allowed to vary. Moreover, only points corresponding to a number of observations larger than 20 are shown. The corresponding duration, t, of the excitation period (period of accelerated strain release) is 36.6 years (1920–1956) for

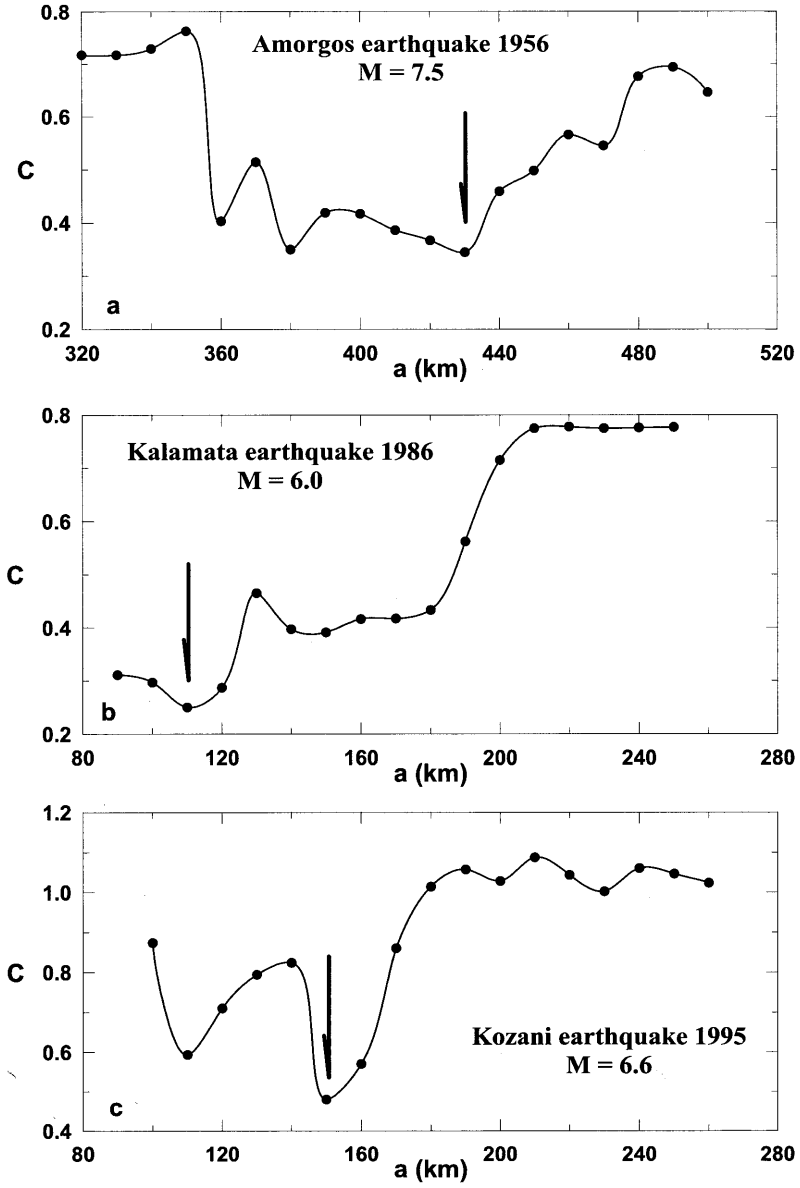

Figure 2
Variation of the parameter C with the length, a (in km), of the maximum axis of the elliptical preshock regions for three destructive earthquakes in the Aegean crust with magnitudes $M = 7.5$, $M = 6.0$ and $M = 6.6$.

the first earthquake, 19.8 years (1967–1986) for the second and 25.5 years (1970–1995) for the third. It is observed that a minimum value of C can be identified for all three cases ($C = 0.35$ for the first, $C = 0.25$ for the second, $C = 48$ for the third),

after which its value most continuously increases with distance. A similar behavior was found for all the other 21 mainshocks examined. The distances (long axis of the ellipse) corresponding to these minima increase with the magnitude of the mainshock (430 km for $M = 7.5$, 150 km for $M = 6.6$, 110 km for $M = 6.0$). For Figures 2b and 2c the distance is truncated at 250–260 km since for larger distances C has mostly constant high values (> 0.7). It is also interesting to note that the identified minimum remains mostly fixed at the same distance even when the time window of the accelerated deformation period is varied within certain limits. This behavior demonstrates that the determined distance, a, is unique (critical) for each mainshock and its determination is very robust. Examination of other solutions with slightly higher C values also shows that the determined critical distance, R, practically varies within a narrow band. The increase of the value of C and its approach to unit for larger than the critical distances is expected because a random distribution of seismicity is observed in such broad areas. It is not, however, easy to explain the increase of the C value for smaller distances, which for certain cases is rather large (see Fig. 2c). It is probable that the seismicity in a part of the region, which is closer to the epicenter of the mainshock, is not accelerated during the excitation period, however this must be checked by further investigation.

Figure 3 shows the corresponding time variation of the observed cumulative Benioff strain in the excitation regions of these three earthquakes (z-e-a are held fixed to their final values), as well as the corresponding curves of the power-law (solid lines) and linear relations (dashed lines) which best fit the data. The data and the best-fit lines shown in all figures are presented only for the finally determined time-period of accelerated deformation, since only for this period were data used for the final determination of the power-law behavior (equation 2). As is expected (from the minimum values of C which are all considerably lower than one) the power-law relation fits well the data, and the corresponding values of the exponent m are much lower than 1 ($m = 0.52$ for the first case, $m = 0.40$ for the second, and $m = 0.54$ for the third).

We must point out that the use of the value of C for the identification of a power-law accelerating energy release behavior (BOWMAN *et al.*, 1998) is performed in a rather strict manner. Equation (2) shows that for $t = t_c$, S equals A, therefore the power-law curve must always pass through the point (t_c, A), which limits its degree of freedom (see solid lines in Fig. 3). On the other hand, the linear fits (dashed lines in Fig. 3) are performed with no constrains. As a result, although both equation (2) and the linear-fit have the same number of unknown parameters, the linear-fit is superior in fitting the data than equation (2), which is the main reason that in several cases C reaches values larger than 1, e.g., Figure 2c. Therefore, the power-law behavior must fit the data substantially better than the linear-fit in order to be selected by the $C < 1$ criterion used in the present study. On the other hand, the use of such strict criteria is necessary in order to achieve the necessary reliability level when detecting accelerating seismicity behavior. It should

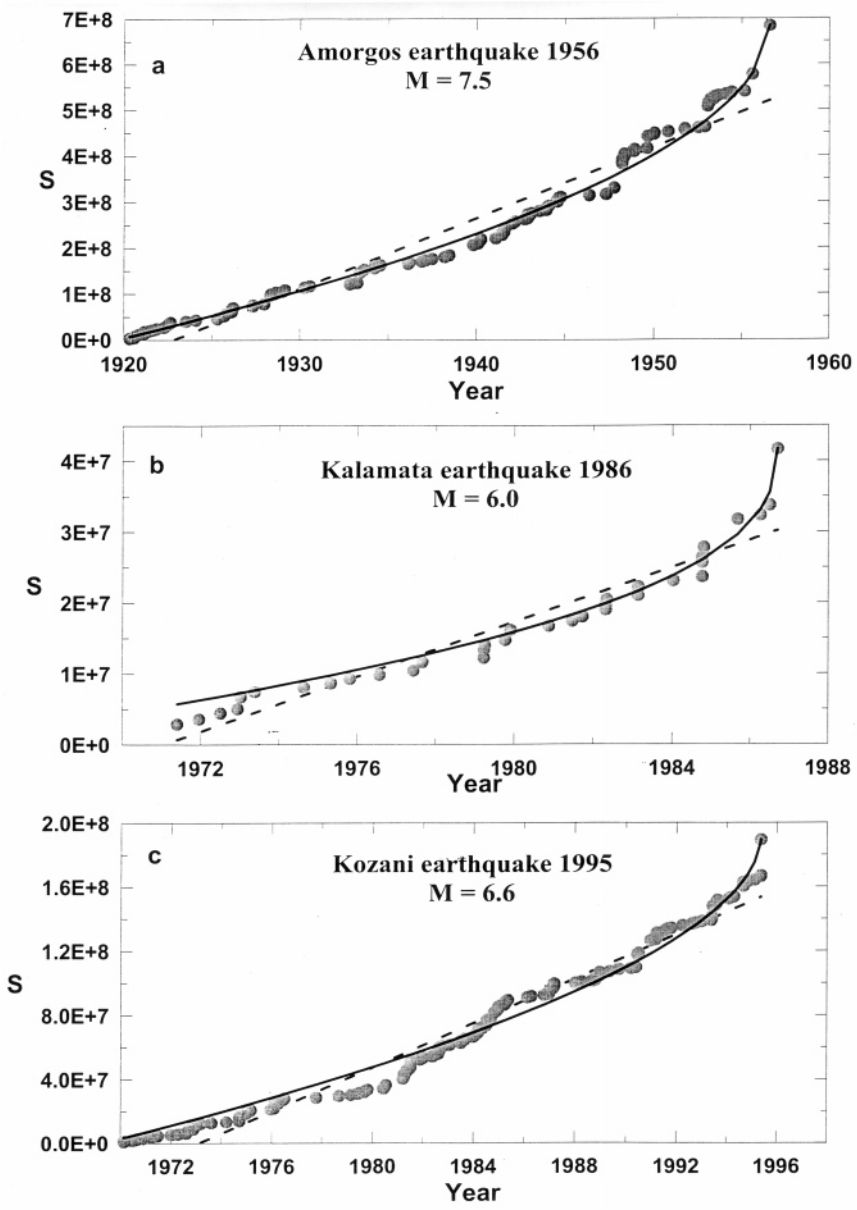

Figure 3
Time variation of the observed cumulative Benioff strain, S (in Joule$^{1/2}$), in the preshock region of the earthquakes which occurred in Amorgos (a), in Kalamata (b) and in Kozani (c). The observations are fitted by a power-law relation in each case (solid line), as well as by a linear relation (dashed line).

also be pointed out that the power-law presented in equation (2) can also be used to identify cases of decelerated, rather than accelerated, Benioff strain release, if values $m > 1$ are defined. However, no such behavior has been found in the studied cases.

Determination of the Model Parameters

The azimuth, z, of the maximum axis, the ellipticity, e, of the preshock area, the radius, R (in km), of the circle with area equal to the corresponding ellipse and the duration, t (in years), of the preshock period for the 24 mainshocks, investigated in this paper are given on the sixth, seventh, eighth and ninth column Table 1. It is observed that in all cases ellipses with quite high ellipticity ($e \geq 0.65$) achieve a better representation of the excited region. The lengths of the maximum axes of the elliptical areas vary between 110 km and 450 km, which are markedly larger than the corresponding dimensions of the rupture (fault) zones.

The next four columns of Table 1 give the values of the exponent, m, of relation (2), the values of the parameter C (minimum value of the ratio of the RMS error of the power-law fit to the RMS error of the linear fit), the number of observations, n (number of preshocks including the mainshock) and the minimum magnitude of preshocks, $M_{\min}$, used to calculate the Benioff strain for each of the 24 cases of mainshocks. The values of m vary between 0.27 and 0.70 and the minimum values of C vary between 0.25 and 0.69, with mean values of $m = 0.47 \pm 0.11$ and $C = 0.49 \pm 0.11$. The number of observations used for each mainshock varies between 31 and 138. The minimum preshock magnitude used in each case is in accordance with the completeness of the data previously defined. The mean Benioff strain rate, s_r, per year for 10^4 km^2 was also calculated for each critical region, using the complete data with $M \geq 5.2$, which occurred during the instrumental period (1911–1998). The calculated values are listed in the last column of Table 1.

Dimension of the Preshock Region

The radius, R, of the circle with an area equal to the corresponding ellipse is considered as a measure of the dimension of the excitation area. Hence, $R = a(1 - e^2)^{1/4}$, where a is the large axis of the elliptical area and e is the ellipticity. Figure 4 shows the variation of R as a function of the magnitude of the mainshock for all twenty-four earthquakes listed on Table 1, denoted by solid diamonds. The following relation is fitted, in the least-squares sense, to the data:

$$\log R = 0.42M - 0.68 \tag{6}$$

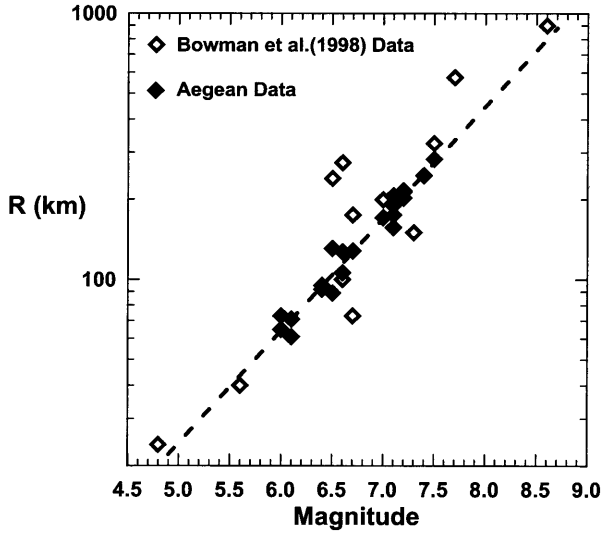

Figure 4
Relation between the radius, R (in km), of the circle with area equal to the elliptical region exhibiting accelerated seismicity and the moment magnitude, M, of the corresponding mainshocks (solid diamonds) for the 24 cases studied in the Aegean area. The independent data set of BOWMAN *et al.* (1998) (open diamonds) is also presented, showing good agreement between the two data sets. The best-fit log R–M relation for the Aegean data is also delineated by dashed-line.

with a correlation coefficient equal to 0.98 and a standard deviation equal to 0.04, shown by the dashed line in Figure 4. In the same plot the results obtained by BOWMAN *et al.* (1998) are presented (open diamonds). A very good agreement can be identified between the two data sets, which suggests that the determined accelerating seismicity behavior has a rather global character. Moreover, it is clear that it is not very difficult to identify this phenomenon, since even using circular areas with approximately defined time-periods for the accelerated seismicity, as in the case of BOWMAN *et al.* (1998), leads to reliable results, as Figure 4 indicates.

PAPAZACHOS and PAPAZACHOU (1997) determined the following relation between the rupture (fault) length, L (in km), and the moment magnitude of shallow earthquakes in the Aegean area:

$$\log L = 0.5M - 1.85. \tag{7}$$

From this relation and equation (6) we find that for our magnitude range ($M = 6.0$–7.5) the half-length fault size $L/2 \simeq R/7.3$–$R/9.6$. Therefore, the dimension of the determined preshock region is about seven ($M = 6.0$) to ten ($M = 7.5$) times the dimension of the fault region.

In Figure 1 two small lines show the orientation of the large axis of each preshock region for each mainshock. Comparison with results previously published for the Aegean area establishes that the determined orientations are in very good

agreement with the direction of the rupture zones identified in the examined area (PAPAZACHOS *et al.*, 1999b), i.e., with the average fault orientation. There are, however, other directions of the large axis of the ellipse for which seismicity also appears to be accelerating, although with higher C values identified. Therefore, although the determined azimuths of the preshock areas seem to correlate with the average fault direction, they should be considered only as indicative for each subregion of the studied area. This indicates that preshock regions have rather complicated shapes and only in a first approximation can be represented by ellipses. It is, however, very important that their spatial extent depends strongly on the magnitude only of the ensuing mainshock.

Duration of Accelerating Benioff Strain

Figure 5 shows the variation of parameter C for three finally determined areas of accelerated deformation (z-e-R are fixed), if we consider different starting years since this accelerated behavior was initiated. Similar to the C-distance variation shown in Figure 2, we can determine the duration, t, of the accelerated Benioff strain release in a region which approaches criticality by considering the starting time which corresponds to the minimum value of parameter C. In. Figure 5 the time variation of parameter C for these preshock regions is shown for the same three destructive earthquakes for which the variation of C with the radius has been presented in Figure 2. Again, only points which correspond to a number of observations larger than 20 are displayed. The beginning of the accelerating seismicity as well as the origin time of the mainshock, defining the duration, t, of the accelerated Benioff strain release, are shown by two arrows in each figure. It should be mentioned that the determined t values are quite robust: Examination of other possible solutions with slightly larger C values than the minimum-C value finally used reveals that the duration of the preshock period is practically invariable for the 24 examined cases.

Examining Figure 5 it is observed that in all three cases the parameter C starts from high values before it reaches its minimum value at the point, which we consider as the starting time of the period of accelerating seismicity. A similar behavior has been observed in all other cases investigated in the present paper. Such variation of C is quite expected: If we examine a long time-period before the main earthquake, the examined region exhibits a more or less random time-distribution of seismicity before the critical phase starts. As soon as we exclude the data before this critical phase initiation, the examined parameter C reaches a minimum value and identifies the start of accelerated Benioff strain release time interval, similar to the cases shown in Figure 3. Figure 5, however, also shows that in all three cases the value of C increases slowly after this minimum and reaches high values after some years, as has been observed for all other cases investigated in this paper. This

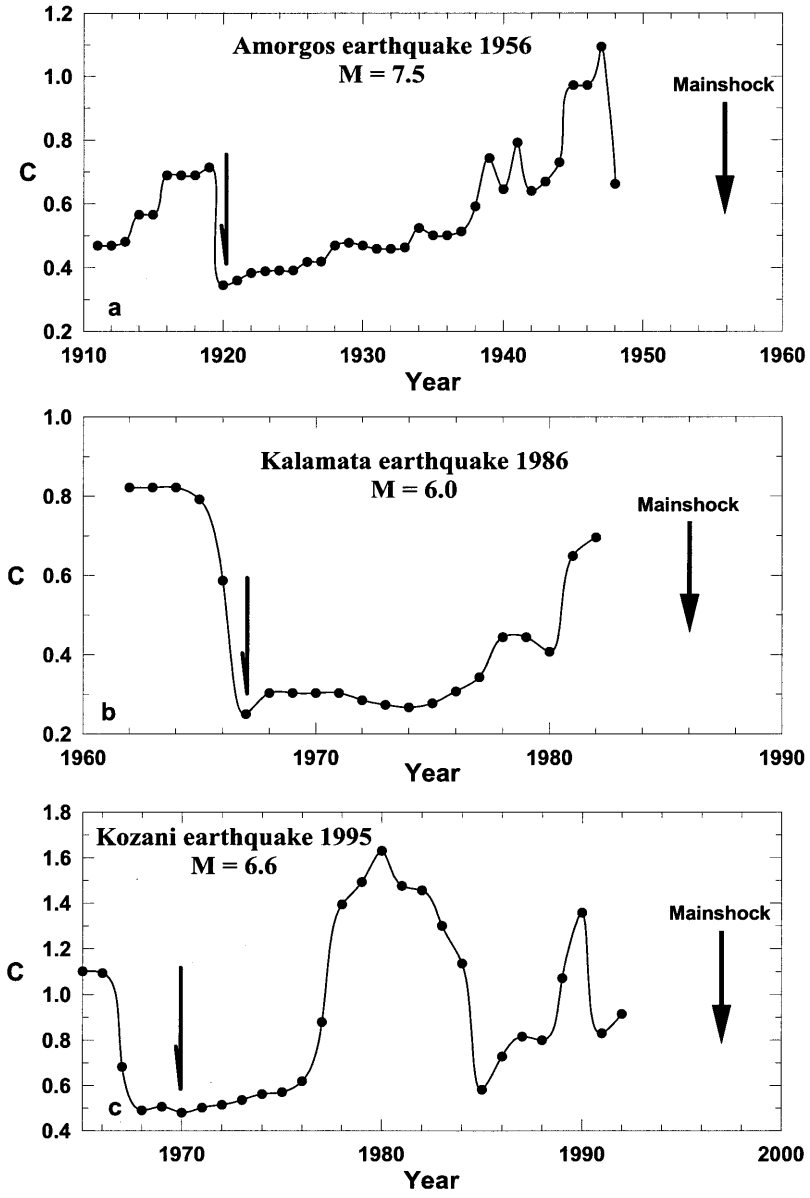

Figure 5
Time variation of the parameter C for the earthquakes of Amorgos (a), Kalamata (b) and Kozani (c).

increase can easily be understood by examining the examples presented in Figure 3: When examining later years as the possible starting time of the initiation of the critical phase, we are essentially removing some of the older data (left part of data plots in Fig. 3) of each $S(t)$-time distribution. Although it is still possible to identify

the presence of accelerated seismicity behavior ($C < 1$), C values gradually increase indicating that this data reduction does not allow discrimination between relation (2) and a linear variation with time. However, if we exclude a significant part of the accelerated seismicity time-period, it becomes impossible to discriminate between accelerated and linear behavior and this is reflected by the significant increase of the obtained C values.

From the information given on Table 1 for the preshock time, t, and the mean Benioff strain rate, s_r (per year for 10^4 km^2) in the preshock area calculated by complete ($M \geq 5.2$) data of the entire instrumental period (1911–1998), the following relation was determined:

$$\log t = 5.94 - 0.75 \log s_r \tag{8}$$

with a correlation coefficient equal to 0.88 and a standard deviation equal to 0.095. The data used for the determination of equation (8), as well as the corresponding best-fit line are presented in Figure 6. This linear dependence of the logarithm of the preshock time on the logarithm of the mean Benioff strain rate (per 10^4 km^2 area) shows that high-seismicity/seismic strain release areas (large $\log s_r$) have smaller preshock times. This indicates that after the critical phase of accelerated behavior starts, the main earthquake will occur faster in these high seismicity areas.

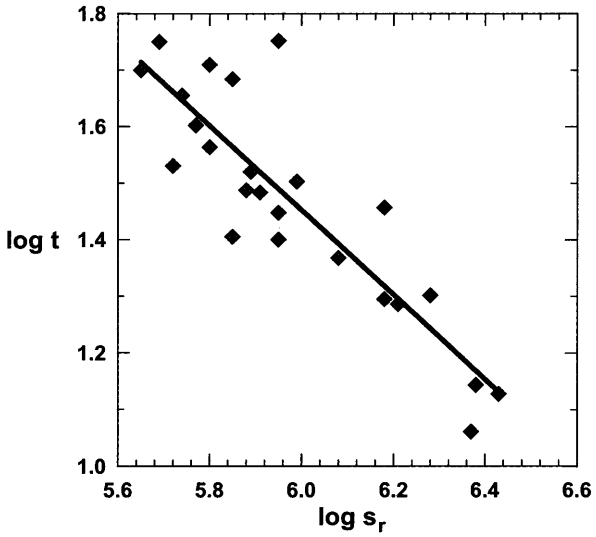

Figure 6
Variation of the logarithm of the time-period of the accelerated seismicity, t, as a function of the logarithm of the average Benioff-strain rate release for $M \geq 5.2$ per year and 10^4 km^2 of the mainshock area. The best-fit line is also shown.

Discussion

Identification of regions in the earth's lithosphere where strain is accelerating before mainshocks, is very important for understanding the geodynamics of the tectonically active part of the lithosphere as well as for practical purposes which concern earthquake prediction and time-dependent seismic hazard assessment. Although identification of such regions improves our knowledge of the regional state of stress, the physical processes, which lead to the accelerating strain release, are not well understood. Possible explanations that have been suggested for the explanation of the accelerated strain energy release before mainshocks are that progressive failure of asperities leads to the concentration of the stress on the remaining locked zones (JONES and MOLNAR, 1979), strain build-up to the mainshock triggers intermediate magnitude earthquakes on surrounding faults (SYKES and JAUMÉ, 1990), creep or flow at depth triggers shallow activity (BUFE and VARNES, 1993), stress flows from smaller faults to intermediate sized faults prior to the mainshock (TURCOTTE, 1999), and that the preshock region is in a critical state which culminates at the generation of the mainshock which is considered as a critical point (SALEUR *et al.*, 1996).

We have seen that preshock regions for the mainshocks with $6.0 \leq M \leq 7.5$ have dimensions about seven to ten times the dimension of rupture (fault) zones where the classical foreshocks and aftershocks occur (relations 6, 7). The larger scatter of the BOWMAN *et al.* (1998) data compared to the Aegean data seen in Figure 4 is easily explained if we consider that: a) BOWMAN *et al.* (1998) used circles, whereas in the present study an extensive search of all possible elliptical areas was performed and, b) the time period, t, of accelerated seismicity was rather arbitrarily selected in their study, whereas in the present work it was defined by a similar search and it follows equation (8).

The identified preshocks last far longer than the classical foreshocks. Therefore, preshocks cannot be explained by elastodynamic interactions, which explains phenomena at the rupture zone (BOWMAN *et al.*, 1998). On the other hand, investigation of seismicity in broad regions of the Aegean crust reveals an accelerating rate of released seismic energy during the last stage of the seismic cycle (KARAKAISIS *et al.*, 1991). Therefore, the preshock time given by relation (8) can be considered as the last part of the interevent time between mainshocks. Once this preshock period starts, equation (8) indicates that the critical phase duration before the main earthquake is smaller for high seismicity areas. This behavior suggests that in high seismicity areas the larger seismic energy release further "accelerates" the end of this phase and the occurrence of the main earthquake.

When the preshock region is identified, relation (6) can be used to estimate the magnitude of the expected mainshock after which its origin time can be estimated by relation (8). Further improvement of these estimations can be made by fitting the observations to a relation of the form of equation (2). Identification of a

preshock region of an expected earthquake on the basis of relation (2) is considerably more difficult for an ensuing earthquake than in the case of an earthquake which took place because in this latter case the parameters t_c (origin time) and A (which depends on the magnitude of the mainshock) of this relation are known. However, these parameters are not known for a future mainshock. There are also difficulties of predicting accurately the epicenter of an ensuing mainshock by this method, because the epicenter can be some distance from the center of the examined preshock region, although our data indicate that this distance is not lengthy.

It is therefore concluded that further work is necessary to better understand the behavior of the tectonically active part of the lithosphere prior to the generation of a mainshock before we endeavor to predict such shocks. In particular, it is necessary to investigate more thoroughly the time and spatial variation of the Benioff strain rate in the preshock region and find methods to more accurately define the boundaries of this region.

Conclusions

The accelerated deformation release before large earthquakes has been studied in the Aegean area. The main modification from previous approaches is the use of elliptical areas within which the time variation of the Benioff strain is examined. The obtained results show that the dimensions of the regions which exhibit a critical behavior increase with the magnitude of the ensuing earthquake, in very good agreement with the recent independent results of BOWMAN *et al*. (1998). Moreover, it is shown that the duration of this critical phase depends on the seismicity level of each area (equation 8), with a shorter duration observed in high seismicity areas. The robustness of the obtained results suggests the possibility of identifying such accelerated behavior before an expected large mainshock, in order to estimate its magnitude and occurrence time.

REFERENCES

ALLÈGRE, C. J., and LE MOUEL, J. L. (1994), *Introduction of Scaling Techniques in Brittle Failure of Rocks*, Phys. Earth Planet Inter. *87*, 85–93.

ANDERSEN, J. V., SORNETTE, D., and LEUNG, K. T. (1997), *Tri-critical Behavior in Rupture Induced by Disorder*, Phys. Rev. Lett. *78*, 2140–2143.

BOWMAN, D. D., OUILLON, G, SAMMIS, C. G., SORNETTE, A., and SORNETTE, D. (1998), *An Observational Test of the Critical Earthquake Concept*, J. Geophys. Res. *103*, 24,359–24,372.

BREHM, D. J., and BRAILE, L. W. (1998), *Application of the Time-to-failure Method for Intermediate-term Prediction in the New Madrid Seismic Zone*, Bull. Seismol. Soc. Am. *88*, 564–580.

BREHM, M. J., and BRAILE, L. W. (1999), *Refinement of the Modified Time-to-failure Method for Intermediate-term Earthquake Prediction*, J. Seismology *3*, 121–138.

BUFE, C. G., and VARNES, D. J. (1993), *Predictive Modelling of the Seismic Cycle of the Great San Francisco Bay Region*, J. Geophys. Res. *98*, 9871–9883.

BUFE, D. G., NISHENKO, S. P., and VARNES, D. J. (1994), *Seismicity Trends and Potential for Large Earthquakes in the Alaska-Aleutian Region*, Pure appl. geophys. *542*, 83–99.

COMNINAKIS, P. E., and PAPAZACHOS, B. C. (1986), *A Catalogue of Earthquakes in Greece and the Surrounding Area for the Period 1901–1985*, Univ. Thessaloniki Geophys. Lab. Publ. *1*, 1–167.

JAUMÉ, S. C., and SYKES, L. R. (1999), *Evolving Towards a Critical Point: A Review of Accelerating Seismic Moment/energy Release Prior to Large and Great Earthquakes*, Pure appl. geophys. *155*, 279–305.

JONES, L. M., and MOLNAR, P. (1979), *Some Characteristics of Foreshocks and Possible Relationship to Earthquake Prediction and Premonitory Slip on Faults*, J. Geophys. Res. *84*, 3596–3608.

KANAMORI, H., MORI, J., HAUKSSON, E., HEATON, T. H., HUTTON, L. K., and JONES, L. M. (1993), *Determination of Earthquake Energy Release and M_L Using Terrascope*, Bull. Seismol. Soc. Am. *83*, 330–346.

KARAKAISIS, G. F., KOUROUZIDIS, M. C., and PAPAZACHOS, B. C. (1991), *Behaviour of seismic activity during a single seismic cycle*. In *Earthquake Prediction: State of the Art* (Strasbourg, France, 15–18 October 1991) pp. 47–54.

KEILIS-BOROK, V. I., KNOPOFF, K., ROTWAIN, I. M., and ALLEN, C. R. (1988), *Intermediate-term Prediction of Occurrence Times of Strong Earthquakes*, Nature *335*, 690–694.

KNOPOFF, L., LEVSHINA, T., KEILIS-BOROK, V. J., and MATTONI, C. (1996), *Increased Long-range Intermediate-magnitude Earthquake Activity Prior to Strong Earthquakes in California*, J. Geophys. Res. Lett. *101*, 5779–5796.

LAMAIGNERE, L., CARMONA, F., and SORNETTE, D. (1996), *Experimental Realization of Critical Thermal Fuse Rupture*, Phys. Res. Lett. *77*, 2738–2741.

LINDH, A. G. (1990), *The Seismic Cycle Pursued*, Nature *348*, 580–581.

MOGI, K. (1969), *Some Features of Recent Seismic Activity in and Near Japan. 2. Activity before and after Great Earthquakes*, Bull. Earthquake Res. Inst. Univ. Tokyo *47*, 395–417.

PAPADOPOULOS, G. A. (1986), *Long-term Earthquake Prediction in the Western Hellenic Arc*, Earthquake Predic. Res. *4*, 131–137.

PAPADOPOULOS, G. A. (1988), *A Note on the Prediction of the September 13, 1986. Strong Earthquake in Kalamata, Southwest Peloponnesus, Greece*, Tectonophysics *145*, 337–341.

PAPAZACHOS, B. C., and PAPAZACHOU, C. B. (1997), *The Earthquake of Greece*, Ziti Editions, Thessaloniki, 304 pp.

PAPAZACHOS, B. C., KIRATZI, A. A., and KARAKOSTAS, B. G. (1997), *Toward a Homogeneous Moment Magnitude Determination in Greece and Surrounding Area*, Bull. Seismol. Soc. Am. *87*, 474–483.

PAPAZACHOS, B. C., PAPADIMITRIOU, E. E., KIRATZI, A. A., PAPAZACHOS, C. B., and LOUVARI, E. K. (1998), *Fault Plane Solutions in the Aegean Sea and the Surrounding Area and their Tectonic Implication*, Boll. Geofis. Teor. Applic. *39*, 199–218.

PAPAZACHOS, B. C., PAPAIOANNOU, CH. A., PAPAZACHOS, C. B., and SAVAIDIS, A. S. (1999a), *A methodology for reliable seismic hazard assessment in the south Balkan area*, EU-Japan Workshop on *Understanding Crustal Processes Leading to Destructive Earthquakes* (Reykjavik, Iceland, June 23–27).

PAPAZACHOS, B. C., PAPAIOANNOU, CH. A., PAPAZACHOS, C. B., and SAVAIDIS, A. S. (1999b), *Rupture Zones in the Aegean Area*, Tectonophysics *308*, 205–221.

RALEIGH, C. B., SIEH, K., SYKES, L. R., and ANDERSON, D. L. (1982), *Forecasting Southern California Earthquakes*, Science *217*, 1097–1104.

SALEUR, H., SAMMIS, C. G., and SORNETTE, D. (1996), *Discrete Invariance, Complex Fractal Dimensions, and Long-periodic Fluctuations in Seismicity*, J. Geophys. Res. *101*, 17,661–17,677.

SORNETTE, A., and SORNETTE, D. (1990), *Earthquake Rupture as a Critical Point. Consequences for Telluric Precursors*, Tectonophysics *179*, 327–334.

SORNETTE, D., and SAMMIS, C. G. (1995), *Critical Exponents from Renormalization Group Theory of Earthquakes: Implications for Earthquake Predictions*, J. Phys. I. *5*, 607–619.

SYKES, L. R., and JAUMÉ, S. (1990), *Seismic Activity on Neighboring Faults as a Long-term Precursor to Large Earthquakes in the San Francisco Bay Area*, Nature *348*, 595–599.

TOCHER, D. (1959), *Seismic history of the San Francisco region*. In *San Francisco Earthquakes of 1957*, (ed. G. B. Oakeshott) CDMG Spec. Rep. 57, pp. 39–48, Calif. Div. Mines Geol., Sacramento.

TURCOTTE, D. L. (1999), *Seismicity and Self-organized Criticality*, Phys. Earth Planet Inter. *111*, 275–293.

VARNES, D. J. (1989), *Predicting Earthquakes by Analyzing Accelerating Precursory Seismic Activity*, Pure appl. geophys. *130*, 661–686.

VANNESTE, C., and SORNETTE, D. (1992), *Dynamics of Rupture in Thermal Fuse Models*, J. Phys. I. Fr. *2*, 1621–1644.

VASSILIOU, M. S., and KANAMORI, H. (1982), *The Energy Release in Earthquakes*, Bull. Seismol. Soc. Am. *72*, 371–387.

(Received July 29, 1999, accepted January 19, 2000)